Journal of Organometallic Chemistry 920 (2020) 121341

Contents lists available at ScienceDirect

Journal of Organometallic Chemistry

journal homepage: www.elsevier.com/locate/jorganchem

Tunable Rh(I) Fischer carbene complexes for application in the hydroformylation of 1-octene

Tshegofatso L. Mashabane [a], G. Kabelo Ramollo [a], George Kleinhans [a], Stephen De Doncker [b], Shepherd Siangwata [b], Manuel A. Fernandes [a], Andreas Lemmerer [a], Gregory S. Smith [b], Daniela I. Bezuidenhout [a, c, *]

[a] Molecular Sciences Institute, School of Chemistry, University of the Witwatersrand, Johannesburg 2050, South Africa
[b] Department of Chemistry, University of Cape Town, 7701, Rondebosch, South Africa
[c] Laboratory of Inorganic Chemistry, Environmental and Chemical Engineering, University of Oulu, P. O. Box 3000, 90014 Oulu, Finland

ARTICLE INFO

Article history:
Received 20 March 2020
Received in revised form
27 April 2020
Accepted 6 May 2020
Available online 16 May 2020

Keywords:
Fischer carbene complexes
Heterometallic complexes
Hydroformylation
p-N,N-dimethylaniline
Ferrocenylcarbene
Ruthenocenyl

ABSTRACT

The preparation of a series of rhodium(I) complexes coordinated by various electronically tuneable Fischer carbene (FC) ligands, is reported. The Rh(I) metal complexes' electronic properties could readily be modulated by variation of a *p-N,N*-dimethylaniline moiety with a ruthenocenyl substituent, or alternatively, substituting the carbene *O*-heteroatom for an amino-group. The electronic properties of the complexes were evaluated, and it was determined from the Tolman electronic parameters that the donor-ability of the FC ligands are comparable to *N*-heterocyclic carbenes. Furthermore, the facile control of the electronic properties of the complexes was demonstrated by mild oxidation of a ferrocenyl aminocarbene rhodium(I) complex, yielding the corresponding ferrocenium rhodium(I) complex cation. Finally, the complexes were evaluated as catalyst precursors for the hydroformylation of 1-octene.

1. Introduction

The use of mono-heteroatom-stabilized Fischer carbene ligands in catalytic applications are still predominantly unexplored, although the exploitation of Fischer carbene complexes (FCCs) in photophysical, optical and sensing applications are on the rise [1]. This dearth in homogeneous catalysis application can mostly be ascribed to the challenges related to the preparation of FCCs of the late transition metals [2], whereby self-dimerisation of the carbene ligand to the corresponding olefin is observed during transmetallation reactions from the group 6 metal FCC precursors [3]. Examples of late transition metal FCCs isolated via this route are therefore not common [4]. This methodology has the benefit of bypassing the requirement for the presence of modifiable carbonyl or isonitrile ligands for nucleophilic attack in traditional Fischer carbene synthesis [5]. Even for the few isolated examples of rhodium(I) FCCs, thermal instability frequently prohibits the use of the complexes in applications requiring elevated temperatures [3]. We have previously found that the use of a donating ferrocenylcarbene ligand of the Fischer-type, was effective towards the preparation of Rh^{I} FCCs, stable to both atmospheric conditions and high temperatures [4a]. More importantly, we could show that these complexes were efficient in catalyzing the hydroformylation of 1-octene. The catalyst selectivity could be modified by variation of both co-ligands (phosphines, phosphites, 1,5-cyclooctadiene (cod), carbonyls or arsines) and Fischer carbene heteroatom substituents (amino-vs alkoxy). The formation of the desired linear aldehyde products could hereby be favoured to yield *n*/iso-aldehyde ratios comparable to those mediated by known rhodium(I) *N*-heterocyclic carbene (NHC) complex catalysts [6]. In this work, we investigate the use of different (hetero)aryl Fischer carbene ligand substituents as an alternative route towards the tailoring of rhodium(I) FCC precatalysts. In particular, the use of metal-containing moieties as carbene substituents are employed as a tool to extend the carbene ligand reactivity beyond what is possible with classic organic (hetero)aryl ring substituents, where for example, an electron-rich ferrocenyl (Fc) or ruthenocenyl (Rc) group could act as

* Corresponding author. Laboratory of Inorganic Chemistry, Environmental and Chemical Engineering, University of Oulu, P. O. Box 3000, 90014 Oulu, Finland.
E-mail address: daniela.bezuidenhout@oulu.fi (D.I. Bezuidenhout).

https://doi.org/10.1016/j.jorganchem.2020.121341

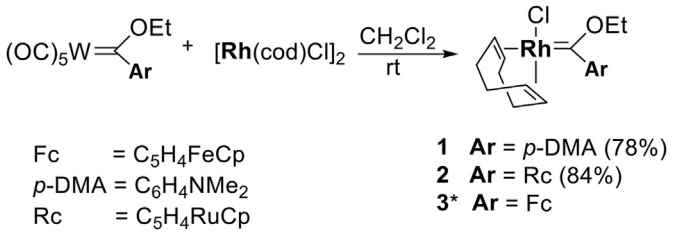

Scheme 1. Synthesis of **1**–**3** via transmetallation from group 6 FCCs. * Complex **3** has been previously reported [4a].

a redox-noninnocent electron reservoir [2d].

2. Results and discussion

2.1. Synthesis and characterization

Pentacarbonyl tungsten(0) ethoxycarbene complexes, containing the strongly electron-donating carbene substituent *p*-*N*,*N*-dimethylaniline (*p*-DMA) [7], or the organometallic ruthenocenyl (Rc) entity [8], were employed as the precursor group 6 FCCs for the preparation of the corresponding Rh^{I} FCCs. [Rh(cod)Cl{C(OEt)*p*-DMA}] (**1**) and [Rh(cod)Cl{C(OEt)Rc}] (**2**) were synthesized (see Scheme 1), following a similar methodology as employed for the analogous complex with a ferrocenyl (Fc) carbene substituent, [Rh(cod)Cl{C(OEt)Fc}] (**3**) (cod = 1,5-cyclooctadiene) [4a]. The carbene transfer reaction ensues with stirring of an equimolar mixture of the group 6 precursor FCC with the dimer $[Rh(cod)Cl]_2$, in dichloromethane at room temperature, while the reaction progress was monitored with thin layer chromatography. Substitution of the cod co-ligand with two carbonyl ligands has previously proven to yield catalyst precursor complexes that are more efficient for the hydroformylation reaction, ascribed to the elimination of the first step of cod-substitution and catalyst activation, amongst other factors [4a]. Thus, complexes **1**–**3** were treated with carbon monoxide to yield the corresponding dicarbonyl complexes **4**–**6** (Scheme 2(a)). Similarly, a simple carbene ligand-modification can also tune the carbene ligand from the more electrophilic alkoxycarbenes to the stronger donor aminocarbenes. Aminolysis of the ethoxycarbenes **1** and **3** with *n*-propylamine yielded complexes **7** [Rh(cod)Cl{C(NH^nPr)*p*-DMA}] and **8** [$Rh(CO)_2$Cl{C(NH^nPr)Fc}], which could be converted to the dicarbonyl analogues **9** [Rh(cod)Cl{C(NH^nPr)*p*-DMA}] and **10** [$Rh(CO)_2$Cl{C(NH^nPr)Fc}], as described above (Scheme 2(a)). The complexes were characterized spectroscopically (see Experimental section 4.2), and a summary of the ^{13}C NMR and FT-IR data is given in Table 1. Upfield shifts, ranging between 19.9 and 21.2 ppm, are seen in the ^{13}C NMR spectra for the carbene carbon atom resonances of the dicarbonyl ethoxycarbene complexes **4**–**6** compared to the cod-precursors **1**–**3**. Similarly, upfield shifts from the carbene carbon resonances of the cod-complexes **7** (252.2 ppm) and **8** (257.9 ppm) to the dicarbonyl aminocarbene-analogues **9** (233.8 ppm) and **10** (237.8 ppm), respectively, are observed (Table 1). As expected, a more marked shielding effect is observed when comparing the aminocarbene derivatives **7**–**10** with their ethoxycarbene precursor complexes **1**, **3**, **4** and **6**, respectively. Upfield shifts ranging from 43.3 to 51.5 ppm are indicative of the increased electron-donation and stabilization from the *N*-heteroatoms towards the electrophilic carbene carbon compared to the ethoxycarbene *O*-heteroatoms [9].

Of interest in this work, however, is the more subtle effect of aryl/metallocenyl carbene substituent variation on the electronic properties of the carbene ligand. As mentioned before, the overall donating ability of the aryl carbene substituent is requisite for the prevention of carbene self-dimerisation. Using the ^{13}C NMR resonances of the different carbene carbon atoms as an indicative tool for the individual carbene ligand electrophilicity, a trend can be established in the order of *p*-DMA < Rc < Fc (compare complex series **1**–**3** and **4**–**6**, Table 1). This is reflected again for the aminocarbene complex series, which excludes the ruthenocenyl substituent for the complexes **7**–**10** (Table 1), where the *p*-DMA carbene substituent consistently leads to higher field carbene carbon atom signals compared to the Fc-analogues. However, the differences are small, and the use of ^{13}C δ ($C_{carbene}$) is not unambiguous.

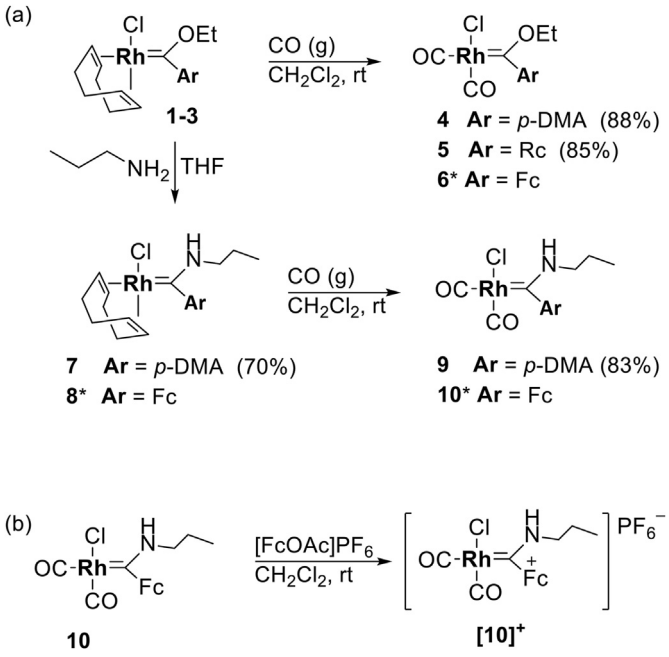

Scheme 2. Preparation of **4**–**10** by (a) post-complexation modifications, and (b) chemical oxidation to yield $[\mathbf{10}]^+$. *The syntheses of these compounds have been previously reported [4a].

Table 1
Spectroscopic data for complexes **1**–**10** and $[\mathbf{10}]^+$.

Complex	^{13}C δ($C_{carbene,\ ppm}$), (^1J(RhC), Hz)	^{13}C δ(CO, ppm), (^1J(RhC), Hz)	IR[a] ν(CO) (cm^{-1})	TEP[b] (cm^{-1})
1	297.9 (d, 43)	–	–	–
2	304.7 (d, 43)	–	–	–
3[e]	309.2 (d, 43)	–	–	–
4	277.1 (d, 37)	187.7 (d, 50)[c] 183.9 (d, 78)[d]	1995[d] 2078[c]	2049
5	283.5 (d, 39)	187.8 (d, 50)[c] 184.2 (d, 76)[d]	2001[d] 2084[c]	2054
6[e]	289.3 (d, 38)	186.5 (d, 50)[c] 182.5 (d, 77)[d]		2054
7	252.2 (d, 40)	–	–	–
8[e]	257.9 (d, 40)	–	–	–
9	233.8 (d, 34)	186.9 (d, 52)[c] 184.2 (d, 78)[d]	2000[d] 2055[c]	2042
10[e]	237.8 (d, 35)	187 (d, 51)[c] 184 (d, 78)[d]		2049
$[\mathbf{10}]^+$	–	–	2018[d] 2089[c]	2063

[a] Recorded in CH_2Cl_2.
[b] Calculated using the linear regression model TEP = $0.8001\nu_{av}(CO)Rh + 420$ cm^{-1} [10b].
[c] CO-ligand *trans* to carbene.
[d] CO-ligand *trans* to Cl.
[e] Previously reported [4a].

Comparison of the Tolman electronic parameters (TEPs) [10] calculated for the [Rh(CO)$_2$Cl{FC}] complexes **4**–**6**, **9** and **10** (Table 1) demonstrate no difference between the ruthenocenyl FC ligand :C(OEt)Rc (**5**) and the ferrocenyl analogue :C(OEt)Fc (**6**). A significant difference of 5–7 cm^{-1} is however observed for the TEPs of *p*-DMA carbene ligands vs Fc carbene ligands (compare 2049 cm^{-1} for :C(OEt)*p*-DMA (**4**) to 2054 cm^{-1} for :C(OEt)Fc (**6**); and 2042 cm^{-1} for :C(NH^{n}Pr)*p*-DMA (**9**) vs 2049 cm^{-1} for :C(NH^{n}Pr)Fc (**10**), Table 1). Interestingly, the TEP value of 2042 cm^{-1} for :C(NH^{n}Pr)*p*-DMA is significantly lower than that described for commonly used NHCs, either saturated or unsaturated (2050–2055 cm^{-1}), as an indicator of the superior σ-donating/lesser π-accepting ability of this monoheteroatom-stabilized carbene ligand [11].

Crystals suitable for single crystal X-ray diffraction were grown from layered hexane/CH_2Cl_2 solutions, for complexes **1**, **2**, **4**, **6**, **7** and **9** (see Fig. 1 and Table 2 for selected bond lengths and angles). The preparation of complex **6** has been previously reported, but the characterization did not include the molecular structure [4a]. In all cases, a (pseudo)square planar geometry is observed for the ligands surrounding the central rhodium(I) ion. In general the O–$C_{carbene}$–C_{Ar} bond angle is smaller for the ethoxy-FCCs **1**, **2**, **4** and **6** (ranging between 110.23(15)°–112.8(2)°), compared to the N–$C_{carbene}$–C_{Ar} bond angles of **7** (116.40(14)°) and **9** (118.42(16)°). This is indicative of the greater sp^2-character of the aminocarbene *N*-atoms, also reflected in the $C_{carbene}$ –N bond lengths of 1.470(2) Å and 1.304(2) Å, for **7** and **9**, respectively, as well as in the markedly longer Rh–$C_{carbene}$ bond lengths for **7** and **9** (2.006(16) Å and 2.0608(18) Å), compared to the analogous ethoxy-FCCs where the Rh–$C_{carbene}$ bond lengths are 1.970(3) Å and 2.046(3) Å, for **1** and **4** respectively.

In addition, the expected effects of cod ligand substitution with two carbonyls are observed, with longer Rh–$C_{carbene}$ bond lengths for the dicarbonyl complexes **4** and **9** (2.046(3) Å and 2.0608(18) Å, respectively), compared to the precursor cod-complexes **1** and **7** (1.970(3) Å and 2.006(16) Å, respectively). However, regardless of the significant electronic differences indicated by the spectroscopic TEPs, the differences in the Rh–$C_{carbene}$ bond lengths for the various carbene aryl substituents are not as marked; compare for example complex **1** with the ruthenocenyl analogue **2** (1.970(3) Å vs 1.953(18) Å), or **4** with the ferrocenyl analogue **6** (2.046(3) Å vs 2.032(2) Å).

2.2. Catalytic studies

Complexes **6**, **8** and **10** were previously screened as catalyst precursors for the hydroformylation reaction [4a], and bear the redox-active ferrocenyl unit as an access point to a carbene ligand for redox-switchable catalysts [12]. This strategy has become an increasingly attractive tool for catalyst tailoring in recent years, and we wanted to exploit this approach to fine-tune the chemo- and regioselectivity performance of the precatalysts. We have previously demonstrated the stability of the oxidized ferrocenium ethoxycarbene ligand, and could isolate the first examples of the radical cations of such ferrocenyl FCCs [13]. The ferrocenyl aminocarbene complex **10** was chemically oxidized using a stoichiometric amount of the oxidizing agent, acetylferrocenium hexafluorophosphate [FcOAc]PF_6 at room temperature in dichloromethane [14]. The suitability of the chemical oxidizing agent was previously determined through cyclic voltammetry experiments, to determine the required oxidation potential [4a].The ferrocenium carbene complex cation **[10]**$^+$ was isolated as the hexafluorophosphate salt. Although recording of the NMR spectra was not possible for this paramagnetic compound (except for the ^{19}F NMR spectrum confirming presence of PF_6 counterion, Appendix A, Fig. S16), the IR stretching frequency of the carbonyl ligands could be measured (Appendix A, Fig. S1), allowing for the calculation of a TEP value of 2063 cm^{-1}. This shift of the absorption bands to higher energy absorption bands (Δ14 cm^{-1} is observed for the TEP of **10** vs **[10]**$^+$), is consistent with the localization of the positive charge on the terminal ferrocenium group, and not on the Rh^I centre bonded directly to the carbonyl ligands [12c,13a,13c]. However, the high-

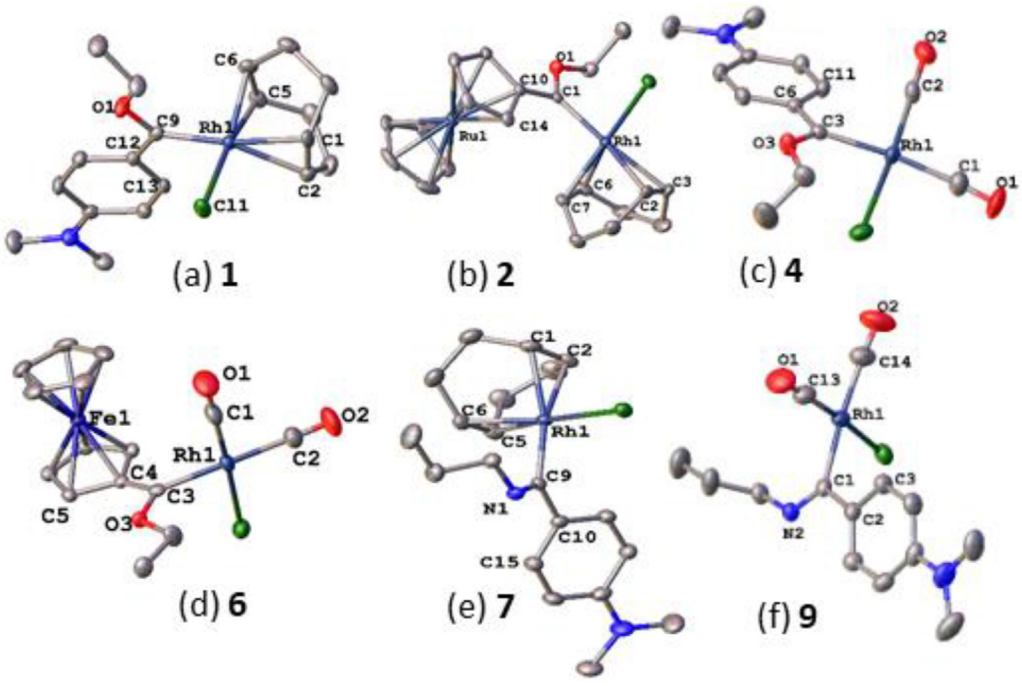

Fig. 1. Solid-state molecular structures of complexes **1**, **2**, **4**, **6**, **7** and **9**. Thermal ellipsoids are shown at 50% probability. Hydrogen atoms are omitted for clarity and a partial atom numbering scheme included.

Table 2
Selected bond lengths (Å) and angles (°).

	1	2	4	6	7	9
Bond Lengths (Å)						
Rh-$C_{carbene}$	1.970(3)	1.953(18)	2.046(3)	2.032(2)	2.006(16)	2.0608(18)
$C_{carbene}$-O/N	1.332(3)	1.311(2)	1.318(3)	1.306(2)	1.470(2)	1.304(2)
$C_{carbene}$-C_{ipso}	1.436(4)	1.451(3)	1.421(4)	1.442(3)	1.307(2)	1.461(2)
Rh—Cl	2.383(8)	2.381(5)	2.353(8)	2.356(6)	2.402(4)	2.3674(5)
Rh—Y[a,b] or Rh-CO_{trans}	2.118(3)[a]	2.159(19)[b]	1.929(3)	1.933(3)	2.219(16)[a]	1.924(2)
Rh—Y[c,d] or Rh-CO_{cis}	1.990(3)[c]	2.002(19)[d]	1.833(3)	1.833(3)	2.106(17)[c]	1.819(2)
Bond Angles (°)						
$C_{carbene}$-Rh-Cl	88.09(8)	87.58(5)	86.02(8)	85.78(6)	89.23(5)	87.35(5)
O/N-$C_{carbene}$-C_{ipso}	111.7(2)	110.23(15)	112.8(2)	111.87(18)	116.40(14)	118.42(16)
Torsion Angles (°)						
C_{α}-C_{ipso}-$C_{carbene}$-O/N	7.79(4)	1.93(3)	4.1(4)	9.1(3)	35.3(3)	12.5(3)

[a] Y = midpoint of C(1)—C(2).
[b] Y = midpoint of C(2)—C(3).
[c] Y = midpoint of C(5)—C(6).
[d] Y = midpoint of C(6)—C(7).

frequency TEP of **[10]**$^+$ unambiguously confirms the weaker donating ability of the oxidized FC-ligand, as expected by the electron-withdrawing nature of the ferrocenium group [13c,15].

The catalytic activity of complexes **1**, **2**, **4**, **5**, **7**, **9** and **[10]**$^+$ in the hydroformylation of 1-octene was evaluated, and compared with the results obtained previously for the ferrocenylcarbene complexes **3**, **6**, **8** and **10**, under the optimized reaction conditions of 40 bar syngas (1:1 CO:H_2) and 75 °C over 4 h (Table 3). Excellent conversions and chemoselectivity were observed for the ethoxycarbene complexes **1**—**3** and **5**, **6**, where the total aldehyde yield exceeded 98% in all cases with complete conversion, with the exception of **4** (79% conversion and 64% total aldehyde yield, respectively, as depicted in Table 3 (entries 1—6)). This is consistent with our previous finding that the more electrophilic ethoxycarbenes show improved chemoselectivity compared to their more stabilized aminocarbene counterparts **7**—**10** [4a]. Moreover, the TOFs reflect the same trend as a measure of the activity of the ethoxycarbene complexes **1**—**3** and **5**, where the TOFs range from 418 to 615 h^{-1}. Correspondingly, the dicarbonyl ethoxycarbene **4** with *p*-DMA carbene substituent displayed the lowest turn-over frequency (TOF = 318 h^{-1}) with the lowest total conversion and aldehyde yield. Notably, comparison of the three aryl ethoxycarbene substituents employed, *p*-DMA, Rc and Fc, shows that both the ruthenocenylcarbene complexes **2** and **5** displayed the highest TOFs (608 h^{-1} and 615 h^{-1}), where the possibility of a secondary, catalytically active Ru^{II} metal centre acting in a synergistic manner with the Rh^{I} catalyst, can not be excluded . However, comparison of the effect of the co-ligands (cod vs dicarbonyl) on either the catalyst activity (TOF and % conversion) or chemoselectivity for aldehyde formation (% total aldehyde yield) is unambiguous. In the case of Rc-substituted FCCs **2** and **5**, replacement of the cod ligand in **2** with two carbonyl ligands in **5**, is accompanied by a slight increase in the activity as the TOF increases from 608 h^{-1} to 615 h^{-1}. This is again consistent with our previous

Table 3
Hydroformylation reaction[a] results obtained from complexes **1**—**10**, and **[10]**$^+$ as catalyst precursors.

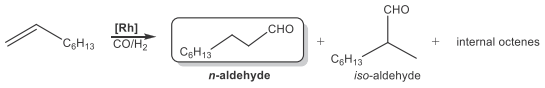

Entry	Catalyst	Conversion (%)	Aldehydes (%)		*Iso*-octenes (%)	TOF[c] (h^{-1})	*n/iso*
			Total aldehydes (%)[b]	Nonanal (%)			
1	**1**	99(1.1)	99 (0.7)	47 (1.1)	1 (0.7)	543 (2.6)	0.89 (0.035)
2	**2**	100	98 (0.6)	47 (1.5)	2 (0.6)	608 (3.8)	0.89 (0.051)
3	**3** [4a]	100	100	44 (4.0)	0	418 (14.2)	0.79 (0.130)
4	**4**	79(10.2)	64 (3.9)	71 (1.1)	36 (3.9)	318 (21.9)	2.44 (0.127)
5	**5**	100	98 (1.3)	47 (2.9)	2 (1.3)	615 (8.8)	0.88 (0.100)
6	**6** [4a]	100	100	50 (1.2)	0	379 (14.1)	0.98 (0.047)
7	**7**	100	82 (4.0)	57 (3.0)	18 (4.0)	512 (26.2)	1.32 (0.160)
8[d]	**7**	100	70 (2.8)	66 (4.3)	30 (2.8)	386 (14.5)	1.95 (0.368)
9	**7** + Hg	100	81 (0.9)	57 (0.2)	19 (0.9)	449 (4.8)	1.31 (0.014)
10	**8**[4a]	100	90 (2.3)	55 (3.0)	10 (2.3)	366 (9.0)	1.25 (0.160)
11	**9**	100	85 (4.0)	56 (3.0)	15 (4.0)	528 (26.2)	1.25 (0.162)
12	**10**[4a]	99(0.1)	85 (0.5)	57 (3.8)	15 (0.5)	343 (8.3)	1.33 (0.210)
13	**[10]**$^+$	55(13.2)	68 (1.8)	69 (0.1)	32 (1.8)	167 (44.6)	2.25 (0.013)

[a] Hydroformylation of 1-octene (6.37 mmol) in toluene (5 mL) at a temperature of 75 C, with syngas (1:1, CO:H_2) at a pressure of 40 bar, a reaction time of 4 hours, and catalyst loading of 5.096 x 10^{-3} mmol. All reactions were performed in either triplicate or duplicate, the average is reported with the standard deviation in parenthesis. Conversions were monitored by gas chromatography, using *n*-decane as an internal standard.
[b] Total aldehydes are a composition of linear and branched aldehydes in a mixture with a percentage sum of 100%.
[c] TOF = (mmol aldehydes per mmol Rh)/time.
[d] Reaction conditions: temperature of 75 C, syngas pressure of 40 bar, a reaction time of 2 hours, and catalyst loading of 5.096 x 10^{-3} mmol.

findings that an overall increase in the electrophilicity of the FCCs result in more active catalyst precursors. However, the opposite trend is observed for the *p*-DMA and Fc FCCs. In these cases, substitution of the cod ligands of **1** and **3** (TOF = 543 and 418 h^{-1}, respectively) coincides with a decrease for the analogous dicarbonyl FCCs **4** and **6** (TOF = 318 and 379 h^{-1}, respectively). In addition, the chemoselectivity for aldehyde formation over internal alkenes, remains virtually unaffected by this co-ligand substitution; except in the case of **4** where the total aldehyde yield significantly decreases from the 99% for its precursor **1**, to 64% for **4**.

In the case of the aminocarbene complexes **7**–**10**, complete conversions are observed (Table 3, entries 7–12), however lower total aldehyde product formation is observed for these catalyst precursors (82–90%), that is indicative of less chemoselective (pre) catalysts with an accompanying increase in regioselectivity (higher *n/iso* values ranging between 1.25 and 1.33). The *n/iso* ratio of the aldehydes range from 0.79 to 0.98 for the ethoxycarbenes **1**–**3**, **5** and **6**, while the least active precatalyst **4** demonstrates the highest overall regioselectivity (2.44, entry 4 Table 3). This again is in accordance with our previous finding that a decrease in chemoselectivity is accompanied by an increase in the regioselectivity for the desired linear aldehydes [4a]. Variation of the reaction time from that of the established optimum 4 h, to half the time (2 h) was done for complex **7** (compare entries 7 and 8, Table 3). As expected, longer reaction time yields a higher % total aldehyde yield (82% vs 70%), as well as an increased TOF (512 h^{-1} vs 386 h^{-1}), but it is accompanied by a significantly lower regioselectivity for the linear aldehyde with an *n/iso* ratio of 1.32 compared to the shorter reaction time where **7** achieves *n/iso* = 1.95 in 2 h.

These results are comparable with analogous rhodium(I) *N*-heterocyclic carbene complexes that displayed TOFs varying between 480 and 3540 h^{-1}, but were accompanied with *n/iso* values lower than 0.5 [16,17]. However, no clear trend could be established between the donating character of the carbene ligands (TEPs) and the TOFs, in isolation of the effect of the co-ligand substitution on the overall electrophilicity of the prepared (pre)catalysts.

The *in situ* chemical oxidation of **10** to **[10]**$^+$ during the catalytic reaction was achieved by addition of a stoichiometric amount of the oxidant acetylferrocenium salt in the reaction vessel. The modification of the carbene ligand to a significantly more electrophilic carbene ligand (*vide supra)* yielded a notably increased regioselectivity result with an *n/iso* ratio of 2.25 (entry 13, Table 3) compared to 1.33 for the neutral precursor **10** (entry 12, Table 3). Again, the increased regioselectivity occurs at the expense of both the chemoselectivity (68% total aldehyde yield) and the activity of the complex (TOF 167 h^{-1}).

A mercury drop-test was performed for **7** with no significant change in either the conversion or the product yields (entry 9, Table 3), compared to the mercury-free reaction (entry 7, Table 3), indicative of a homogeneous catalyst mode-of-action [18].

3. Conclusions

In summary, new examples of electronically tuneable and thermally stable Rh^I FCCs were isolated, with the electronic properties modulated by the variation of electron-donating aryl carbene substituents, *p*-*N*,*N*-dimethylaniline and ruthenocenyl. Exploitation of the redox activity of the ferrocenyl FC ligand was achieved by chemical oxidation to modulate catalytic performance. The performance of these complexes as precatalysts for 1-octene hydroformylation was compared to the previously evaluated ferrocenylcarbene analogues. The carbene ligand modification yielded catalysts with higher TOFs in the case of the ruthenocenyl FCCs **2** and **5**, while the highest regioselectivity was achieved for the *p*-DMA FCC **4**.

4. Experimental

4.1. Methods and materials

The preparation, purification and reactions of the complexes described were carried out under an atmosphere of dry, oxygen-free N_2 or Ar gas using standard Schlenk techniques. All reactions were mechanically stirred and monitored by IR spectroscopy where relevant. The precursors $[W(CO)_5\{C(OEt)Ar\}]$ [Ar = *p*-DMA [7], Fc [4a], Rc [8]] and $[Rh(cod)Cl]_2$ were prepared according to literature procedures. Preparation of the rhodium carbene complexes **3**, **6**, **8**, and **10** has previously been reported by our research group [4a]. Aluminum oxide 60 (particle size 0.05–0.15 mm) was used as resin for all column chromatography separations. Anhydrous tetrahydrofuran (THF), diethyl ether (Et_2O), and *n*-hexane were distilled over sodium metal and dichloromethane (DCM) was distilled over CaH_2. All other reagents are commercially available and were used as received.

Nuclear magnetic resonance (NMR) spectra were recorded on Bruker Avance–III–400 and Bruker Avance–III–500 spectrometers using $CDCl_3$, CD_2Cl_2, and C_6D_6 as solvents at 25 °C. The NMR spectra were recorded for ^1H at 400.13 and 500.13 MHz, and for ^{13}C at 100.63 and 125.78 MHz. The ^{19}F NMR spectrum of complex **[10]**$^+$ was recorded at 376.46 MHz. Infrared spectroscopy was performed on a PerkinElmer Spectrum FT-IR spectrophotometer over the range 3600–1600 cm^{-1}. Solution IR spectra were recorded in CH_2Cl_2 using a NaCl cell with a path length of ca. 1.0 mm. Melting points were measured with a Stuart SMP10 melting point apparatus.

All crystals for single-crystal X-ray diffraction were grown by slow diffusion of *n*-hexane into a concentrated CH_2Cl_2 solution of the carbene complex at 4 °C. Single crystal X-ray diffraction data for complexes **1**, **2** and **4** were collected at 173 K (**1**, **4, 6**, **7** and **9**) or at 150 K (**2**), on a Bruker Apex II CCD diffractometer (**1, 6**, **7**, **6**, **7**, **9**), while data for complexes **2** and **4** were collected using a Bruker Venture D8 Photon CMOS diffractometer, with a graphite-monochromated Mo-K_α (λ = 0.71073 Å) radiation using an Oxford Cryostream 600 cooler. All data reductions were carried out using the program SAINT+, version 6.02 [19] and empirical absorption corrections were made using SADABS [19]. Space group assignments were made using *XPREP* [19]. The structures were solved in the *WinGX* [20] Suite of programs, using intrinsic phasing through *SHELXT* [21] and refined using full-matrix least-squares/difference Fourier techniques on F^2 using *SHELXL-2017* [21]. All C-bound H atoms were placed at idealized positions and refined as riding atoms with isotropic parameters 1.2 times those of their parent atoms. All diagrams and publication material were generated using OLEX2, *ORTEP-3* [20] and *PLATON* [22]. Experimental details of the X-Ray analyses are provided in Table S1.

Mass spectral analyses were performed on a Bruker Compact Q-TOF mass spectrometer (Bruker Daltonics, Bremen, Germany) with a positive electron spray as the ionization technique by direct infusion at 0.3 mL min^{-1}. The *m/z* values were measured in the range of 50–1000 in acetonitrile. Prior to analysis, the instrument was calibrated with sodium formate (5 mM) in resolution mode. Elemental analyses were carried out using an Elementar vario-ELcube CHNS–O analyser.

The hydroformylation reactions were carried out in duplicates or triplicates, in 90 mL stainless steel pipe reactors. Each reactor was charged with the catalyst precursor (5.096×10^{-3} mmol), the substrate: 1-octene (0.805 g, 7.175 mmol), and the internal standard: *n*-decane (0.204 g, 1.435 mmol) all dissolved in toluene (5 mL). The reactor was sealed, purged three times with N_2 (g) and twice with syngas (1:1, CO/H_2) before heating to the desired temperature, under the desired syngas pressure. Once the reaction time

was reached, the reactor was depressurized and the reaction mixture was allowed to cool to room temperature before analysing using gas chromatography. Authentic aldehyde and iso-octene standards were used for the confirmation of the products afforded.

4.2. Experimental synthetic procedures

[Rh(cod)Cl{C(OEt)*p*-DMA}], 1. A mixture of [W(CO)$_5${C(OEt)*p*-DMA}] (0.500 g, 1.0 mmol, 2.00 eq.) and [Rh(cod)Cl]$_2$ (0.247 g, 0.50 mmol, 1.00 eq.) in deoxygenated CH_2Cl_2 (10 mL) was stirred for 3 days at room temperature. The resulting brown solution was reduced *in vacuo* and added to an aluminium oxide chromatography column. Elution with CH_2Cl_2 gave a yellow band, which was collected and evaporated to dryness, resulting in a yellow powder. Yield = 0.165 g, 78%. Mp: 156–157 °C. **^{1}H-NMR** (500 MHz, CD_2Cl_2) δ 8.40 (d, br, $^3J_{HH}$ = 8.6 Hz, 2H, DMA-H$_{\alpha,\alpha'}$), 6.68 (d, $^3J_{HH}$ = 8.8 Hz, 2H, DMA-H$_{\beta,\beta'}$), 5.90 (dq, $^2J_{HH}$ = 14.1, $^3J_{HH}$ = 7.4 Hz, 1H, OCH$_2$CH$_3$), 5.66 (dq, $^2J_{HH}$ = 13.9, $^3J_{HH}$ = 7.5 Hz, 1H, OCH$_2$CH$_3$), 5.27–5.24 (m, 1H, cod-CH), 5.15–5.10 (m, 1H, cod-CH), 3.27–3.23 (m, 2H, cod-CH), 3.10 (s, 6H, N(CH$_3$)$_2$), 2.56–2.29 (m, 4H, cod-CH$_2$), 2.14–1.97 (m, 4H, cod-CH$_2$), 1.65 (t, $^3J_{HH}$ = 7.2 Hz, 3H, OCH$_2$CH$_3$). **^{13}C-NMR** (126 MHz, CD_2Cl_2) δ 297.9 (d, $^1J_{RhC}$ = 43.0 Hz, C$_{carbene}$), 155.1 (C$_q$), 132.9 (d, $^2J_{RhC}$ = 2.2 Hz, C$_{ipso}$), n.o. (DMA-C$_{\alpha,\alpha'}$), 110.7 (DMA-C$_{\beta,\beta'}$), 106.3 (d, $^1J_{RhC}$ = 4.9 Hz, cod-CH), 105.9 (d, $^1J_{RhC}$ = 4.6 Hz, cod-CH), 77.2 (OCH$_2$CH$_3$), 73.0 (d, $^1J_{RhC}$ = 15.0 Hz, cod-CH), 67.9 (d, $^1J_{RhC}$ = 14.8 Hz, cod-CH), 40.5 (N(CH$_3$)$_2$), 33.5 (cod-CH$_2$), 32.9 (cod-CH$_2$), 29.0 (cod-CH$_2$), 28.5, (cod-CH$_2$), 15.6 (OCH$_2$CH$_3$). **ESI-MS**: (*m*/*z*) calcd for $C_{19}H_{27}ONRh^+$: 388.1148 [M – Cl]$^+$; found 388.1146; elemental analysis calcd (%) for $C_{19}H_{27}ONClRh$: C 53.85, H 6.42, N 3.31. Found: C 53.89, H 6.40, N 3.24.

[Rh(cod)Cl{C(OEt)Rc}], 2. This complex was prepared similarly from [W(CO)$_5$Cl{C(OEt)Rc}] (0.250 g, 0.41 mmol, 2.00 eq.) and [Rh(cod)Cl]$_2$ (0.101 g, 0.21 mmol, 1.00 eq.). The reaction was stirred for 8 days to allow for complete conversion of the starting materials. The product was isolated as an orange powder. Yield = 0.185 g, 84%. Mp: 119–120 °C. **^{1}H-NMR** (300 MHz, $CDCl_3$) δ 5.81 (dq, $^2J_{HH}$ = 10.2 Hz, $^3J_{HH}$ = 7.1 Hz, 1H, OCH$_2$CH$_3$), 5.49 (dq,$^2J_{HH}$ = 10.4 Hz, $^3J_{HH}$ = 7.1 Hz, 1H, OCH$_2$CH$_3$), 5.43–5.42 (m, 1H, RuCp'), 5.33–5.27 (m, 1H, cod-CH), 5.27 (s, 1H, RuCp'), 5.18–5.11 (m, 1H, cod-CH), 4.93–4.91 (m, 1H, RuCp'), 4.89–4.87 (m, 1H, RuCp'), 4.64 (s, 5H, RuCp), 3.60–3.55 (m, 1H, cod-CH), 3.31–3.26 (m, 1H, cod-CH), 2.58–1.90 (m, 8H, cod-CH$_2$), 1.54 (t, $^3J_{HH}$ = 7.1 Hz, 3H, OCH$_2$CH$_3$). **^{13}C NMR** (75 MHz, $CDCl_3$) δ 304.7 (d, $^2J_{RhC}$ = 43.3 Hz, C$_{carbene}$), 106.9 (d, $^2J_{RhC}$ = 4.5 Hz, cod-CH), 106.6 (d,$^2J_{RhC}$ = 4.4 Hz, cod-CH), 91.5 (d, $^3J_{RhC}$ = 1.8 Hz, RuCp'-C$_{ipso}$), 77.9 (OCH$_2$CH$_3$), 75.3 (RuCp'), 74.9 (RuCp '), 74.5 (d, $^2J_{RhC}$ = 14.7 Hz, cod-CH), 72.3 (RuCp), 67.9 (d, $^2J_{RhC}$ = 14.9 Hz, cod-CH), 33.8 (cod-CH$_2$), 32.1 (cod-CH$_2$), 28.9 (cod-CH$_2$), 27.6 (cod-CH$_2$), 15.3 (OCH$_2$CH$_3$). **ESI-MS:** (*m*/*z*) calcd for $C_{21}H_{26}ORuRh^+$: 449.0082 [M – Cl]$^+$; found 449.0085; elemental analysis calcd for $C_{21}H_{26}OClRuRh$: C 47.25, H 4.91. Found: C 47.15, H 4.90.

[Rh(CO)$_2$Cl{C(OEt)*p*-DMA}], 4. Carbon monoxide gas was bubbled for 5 min through a stirred solution of **1** (0.050 g, 0.11 mmol, 1.00 eq.) in CH_2Cl_2 (10 mL) in the absence of light and at room temperature. An immediate colour change from orange to pale-yellow was observed. The flow of CO was stopped, and golden crystals were grown by slow diffusion of *n*-hexane (2 mL) into the concentrated CH_2Cl_2 reaction mixture at −30 °C. Yield = 0.035 g, 86%. Mp: 116–118 °C. **^{1}H-NMR** (400 MHz, CD_2Cl_2) δ 8.32 (s, 2H, DMA-H$_{\alpha,\alpha'}$), 6.70 (d, $^3J_{HH}$ = 9.7 Hz, 2H, DMA-H$_{\beta,\beta'}$), 5.41–5.35 (m, 2H, OCH$_2$CH$_3$), 3.17 (s, 6H, N(CH$_3$)$_2$), 1.61 (t, $^3J_{HH}$ = 7.1 Hz, 3H, OCH$_2$CH$_3$). **^{13}C-NMR** (101 MHz, CD_2Cl_2) δ 277.1 (d, $^1J_{RhC}$ = 36.9 Hz, C$_{carbene}$), 187.7 (d, $^1J_{RhC}$ = 50.0 Hz, CO), 183.9 (d, $^1J_{RhC}$ = 77.7 Hz, CO), 157.1 (C$_q$), 131.9 (d, $^2J_{RhC}$ = 2.3 Hz, C$_{ipso}$), n.o. (DMA-C$_{\alpha,\alpha'}$), 111.2 (DMA-C$_{\beta,\beta'}$), 79.5 (d, $^3J_{RhC}$ = 1.7 Hz, OCH$_2$CH$_3$), 40.7 (N(CH$_3$)$_2$), 15.1 (OCH$_2$CH$_3$). **IR** (NaCl, cm^{-1}): 1995(m), 2078(m). **ESI-MS:** (*m*/*z*) calcd for $C_{12}H_{15}O_2NRh^+$: 308.0158 [M – Cl - CO]$^+$; found 308.0155; elemental analysis calcd for $C_{13}H_{15}O_3NClRh$: C 42.02, H 4.07, N 3.77. Found: C 42.08, H 4.09, N 3.69.

[Rh(CO)$_2$Cl{C(OEt)Rc}], 5 Similarly, this complex was synthesized from **2** (0.050 g, 0.09 mmol, 1.00 eq.). The product was isolated as yellow fine crystals. Yield = 0.038 g, 88%. Mp: 98–101 °C. **^{1}H-NMR** (400 MHz, C_6D_6) δ 5.31 (s, br, 1H, RuCp'), 5.21 (s, br, 1H, RuCp'), 5.13 (dq, $^2J_{HH}$ = 14.3, $^3J_{HH}$ = 7.3 Hz, 1H, OCH$_2$CH$_3$), 4.92 (dq, $^2J_{HH}$ = 14.0, $^3J_{HH}$ = 7.4 Hz, 1H, OCH$_2$CH$_3$), 4.56–4.55 (m, 2H, RuCp'), 4.54 (s, 5H, RuCp), 1.04 (t, $^3J_{HH}$ = 7.1 Hz, 3H, OCH$_2$CH$_3$). **^{13}C-NMR** (101 MHz, C_6D_6) δ 283.5 (d, $^1J_{RhC}$ = 38.6 Hz, C$_{carbene}$), 187.8 (d, $^1J_{RhC}$ = 49.9 Hz, CO$_{trans}$), 184.2 (d, $^1J_{RhC}$ = 75.8 Hz, CO$_{cis}$), 92.0 (d, $^2J_{RhC}$ = 2.8 Hz, C$_{ipso}$), 80.6 (d, $^3J_{RhC}$ = 1.8 Hz, OCH$_2$CH$_3$), 77.3 (RuCp'), 76.9 (RuCp'), 73.9 (RuCp), 14.3 (OCH$_2$CH$_3$). IR (NaCl, cm^{-1}): 2001(m), 2084(m). **ESI-MS:** (*m*/*z*) calcd for $C_{14}H_{14}O_2ClRuRh^+$: 418.9041 [M – Cl - CO]$^+$; 418.9021; elemental analysis calcd for $C_{15}H_{14}O_3ClRuRh$: C 37.40, H 2.93. Found: C 36.95, H 3.01.

[Rh(cod)Cl{C(NH^{n}Pr)*p*-DMA}], 7. 1 (0.20 g, 0.52 mmol, 1.00 eq.) was dissolved in degassed THF. ^{n}PrNH$_2$ (0.17 mL, 2.08 mmol, 4.00 eq.) was added dropwise and the solution stirred for 1 hr. The volatiles were removed under reduced pressure and the product was washed with n-hexane, extracted in CH_2Cl_2, and the solvent removed under reduced pressure before drying under vacuum overnight. The residue was dissolved in minimum CH_2Cl_2 for slow diffusion with *n*-hexane, to afford an orange powder. Yield = 0.145 g, 70%. Mp (dec): 163–165 C. **^{1}H-NMR** (400 MHz, CD_2Cl_2) δ 8.19 (s, br, 1H, NHCH$_2$CH$_2$CH$_3$), 7.99 (d, $^3J_{HH}$ = 9.0 Hz, 2H, DMA-H$_{\alpha,\alpha'}$), 6.71 (d, $^3J_{HH}$ = 9.0 Hz, 2H, DMA-H$_{\beta,\beta'}$), 5.06–4.84 (m, 2H, cod-CH), 4.53 (t, $^3J_{HH}$ = 6.0 Hz, 2H, NHCH$_2$CH$_2$CH$_3$), 3.25–3.27 (m, 1H, cod-CH), 3.11–3.05 (m, 1H, cod-CH), 3.04 (s, 6H, N(CH$_3$)$_2$), 2.44–2.37 (m, 2H, cod-CH), 2.33–2.28 (m, 1H, cod-CH), 1.94–1.65 (m, 5H, cod-CH$_2$, NHCH$_2$CH$_2$CH$_3$), 1.11 (t, $^3J_{HH}$ = 7.4 Hz, 3H, NHCH$_2$CH$_2$CH$_3$). **^{13}C-NMR** (101 MHz, CD_2Cl_2) δ 252.2 (d, $^1J_{RhC}$ = 40.0 Hz, C$_{carbene}$), 153.3 (C$_q$), 130.3 (DMA-C$_{\alpha,\alpha'}$), 128.9 (C$_{ipso}$), 111.3 (DMA-C$_{\beta,\beta'}$), 100.6 (d, $^1J_{HH}$ = 6.0 Hz, cod-CH), 100.1 (d, $^1J_{HH}$ = 5.8 Hz, cod-CH), 71.6 (d, $^1J_{RhC}$ = 15.2, cod-CH), 68.1 (d, $^1J_{RhC}$ = 15.0, cod-CH), 55.8 (NHCH$_2$CH$_2$CH$_3$), 40.4 (N(CH$_3$)$_2$), 33.4 (cod-CH$_2$), 32.9 (cod-CH$_2$), 29.2 (cod-CH$_2$), 28.6 (cod-CH$_2$), 23.6 (NHCH$_2$CH$_2$CH$_3$), 11.9 (NHCH$_2$CH$_2$CH$_3$). **IR** (NaCl, cm^{-1}): 3288. **ESI-MS**: (*m*/*z*) calcd for $C_{20}H_{30}ON_2Rh^+$: 389.1463 [M – Cl]$^+$; found 389.2205.

[Rh(CO)$_2$Cl{C(NH^{n}Pr)*p*-DMA}], 9. 7 (0.80 g, 0.19 mmol, 1.0 eq.) was dissolved in degassed THF (5 mL) and purged with CO (g) for 15 min in the absence of light. The solution was allowed to stir for a further 30 min in CO (g) atmosphere, before the removal of volatiles under reduced pressure. The orange residue was washed with *n*-hexane, extracted in CH_2Cl_2, and concentrated in *vacuo*; before slow diffusion into *n*-hexane, affording dark orange crystals. Yield (0.072 g, 0.185 mmol). Mp: 119–121 C. **^{1}H-NMR** (500 MHz, CD_2Cl_2) δ 8.53 (s, br, 1H, NHCH$_2$CH$_2$CH$_3$), 7.91 (d, $^3J_{HH}$ = 9.1 Hz, 2H, DMA-H$_{\alpha,\alpha'}$), 6.70 (d, ^3J(HH) = 9.1 Hz, 2H, DMA-H$_{\beta,\beta'}$), 4.29 (br s, 1H, NHCH$_2$CH$_2$CH$_3$), 4.10 (br s, 1H, NHCH$_2$CH$_2$CH$_3$), 3.07 (s, 6H, N(CH$_3$)$_2$), 1.86 (br s, 2H, NHCH$_2$CH$_2$CH$_3$), 1.06 (t, $^3J_{HH}$ = 7.4 Hz, 3H, NHCH$_2$CH$_2$CH$_3$). **^{13}C-NMR** (126 MHz, CD_2Cl_2) δ 233.8 (d, $^1J_{RhC}$ = 34.3 Hz, C$_{carbene}$), 187.8 (d, $^1J_{RhC}$ = 51.5 Hz, CO$_{trans}$), 184.3 (d, $^1J_{RhC}$ = 77.9 Hz, CO$_{cis}$), 154.3 (C$_q$), 132.3 (DMA-C$_{\alpha,\alpha'}$), 128.1 (C$_{ipso}$), 111.3 (DMA-C$_{\beta,\beta'}$), 56.6 (d, $^3J_{RhC}$ = 1.7 Hz, NHCH$_2$CH$_2$CH$_3$), 40.4 (N(CH$_3$)$_2$), 23.1 (NHCH$_2$CH$_2$CH$_3$), 11.6 (NHCH$_2$CH$_2$CH$_3$). **IR** (CH_2Cl_2, ν(CO) and ν(NH), cm^{-1}): 2000, 2055, 3303. ESI-MS: (*m*/*z*) calcd for $C_{13}H_{18}ON_2Rh^+$: 321.0474 [M – Cl - CO]$^+$; found 321.0235.

[Rh(CO)$_2$Cl{C(NH^{n}Pr)Fc}][PF$_6$], [10]$^+$. A mixture of [Rh(CO)$_2$Cl{C(NH^{n}Pr)Fc}] (**10**) (0.020 g, 0.04 mmol, 1.00 eq.) and [FcCOCH$_3$]$^+$[PF$_6$]$^-$ (0.021 g, 0.06 mmol, 1.10 eq.) was dissolved in deoxygenated CH_2Cl_2 (5 mL) at room temperature and stirred for

24 h. The resulting brown solution was evaporated to dryness *in vacuo*, then washed with diethyl ether, and extracted with CH_2Cl_2 via cannula filtration. Slow concentration of the CH_2Cl_2 solution under reduced pressure gave a brown powder. Yield = 0.019 g, 73%. Mp: 142–143 °C. **^{19}F-NMR** (376 MHz, CD_2Cl_2) δ −82.6 (d, $^1J_{PF}$ = 712.9 Hz, PF_6). **IR** (NaCl, ν(CO) and ν(NH), cm^{-1}): 2018, 2089, 3306.

Declaration of competing interest

Authors do not have any conflicts of interest to declare.

Acknowledgements

The authors gratefully acknowledge the National Research Foundation, South Africa (NRF 115642; NRF 94784; NRF 100119; NRF 111705, NRF-DST Centre of Excellence in Catalysis – c* change (G.S·S)) and Sasol Technology R&D Pty. Ltd. (South Africa) for financial support (D.I·B).

Appendix A. Supplementary data

Supplementary data to this article can be found online at https://doi.org/10.1016/j.jorganchem.2020.121341.

References

[1] a) R.E. Lazo-Jimenez, M.C. Ortega-Alfaro, J.G. Lopez-Cortes, C. Alvarez-Toledano, J.A. Chavez-Carvayar, J. Ignes-Mullol, M. Gonzalez-Torres, P. Carreon-Castro, Materials 9 (2016) 167;
b) P. Srivastava, M. Ghasemi, N. Ray, A. Sarkar, J. Kocabova, S. Lachmanova, M. Hromadova, S. Boujday, S. Cauteruccio, P. Thakare, E. Licandro, C. Fosse, M. Salmain, Appl. Surf. Sci. 385 (2016) 47–55;
c) M.C. Bertolino, A.M. Granados, Appl. Surf. Sci. 383 (2016) 375–381;
d) R.L. Arrowsmith, A.J. Atkin, S.W. Botchway, I.J.S. Fairlamb, J.M. Lynnam, J.W.B. Moir, S.I. Pascu, J.S. Ward, W.-Q. Zhang, Dalton Trans. 44 (2015) 4957–4962;
e) J.S. Ponniah, S.K. Barik, A. Thakur, R. Ganesamoorth, S. Ghosh, Organometallics 33 (2014) 3096–3107.
[2] a) K. Skoch, I. Cisarova, F. Uhlik, P. Stepnicka, Dalton Trans. 47 (2018) 16082–16101;
b) D. Munz, Organometallics 37 (2018) 275–289;
c) H.G. Raubenheimer, Dalton Trans. 43 (2014) 16959–16973;
d) D.I. Bezuidenhout, S. Lotz, D.C. Liles, B. van der Westhuizen, Coord. Chem. Rev. 256 (2012) 479–524;
e) W.I. Dzik, X.P. Zhang, B. de Bruin, Inorg. Chem. 50 (2011) 9896–9903;
f) I. Fernandez, F.P. Cossio, M.A. Sierra, Acc. Chem. Res. 44 (2011) 479–490;
g) Fernandez-Rodriguez, P. Garcia-Garcia, E. Aguilar, Chem. Commun. 46 (2010) 7670–7687;
h) K.H. Dotz, J. Stendel Jr., Chem. Rev. 109 (2009) 3227–3274;
i) J. Barluenga, J. Santamaria, M. Tomas, Chem. Rev. 104 (2004) 2259–2284.
[3] a) M. Gomez-Gallego, M.J. Mancheno, M.A. Sierra, Acc. Chem. Res. 38 (2005) 44–53;
b) I. Fernandez, M.J. Mancheno, R. Vicente, L.A. Lopez, M.A. Sierra, Chem. Eur J. 14 (2008) 11222–11230.
[4] a) G.K. Ramollo, M.J. Lopez-Gomez, D.C. Liles, L.C. Matsinha, G.S. Smith, D.I. Bezuidenhout, Organometallics 34 (2015) 5745–5753;
b) J. Barluenga, R. Vicente, L.A. Lopez, M. Tomas, J. Organomet. Chem. 691 (2006) 5642–5647;
c) J. Barluenga, R. Vicente, L.A. Lopez, E. Rubio, M. Tomas, C. Alvarez-Rua, J. Am. Chem. Soc. 126 (2004) 470–471;
d) I. Gottker-Schnetmann, R. Aumann, K. Bergander, Organometallics 20 (2001) 3574–3581.
[5] E.O. Fischer, A. Maasbol, Angew. Chem. Int. Ed. 3 (1964) 580–581.
[6] a) W. Gil, A.M. Trzeciak, Coord. Chem. Rev. 255 (2011) 473–483;
b) A. R. Almeida, A. F. Peixoto, M. J. F. Calvete, P. M. P. Gois, M. M. Pereira, 2011, 8, 764-775;. c) S. Díez-González, N. Marion, S.P. Nolan, Chem. Rev. 109 (2009) 3612–3676;
d) J.M. Praetorius, C.M. Crudden, Dalton Trans. (2008) 4079–4094;
e) A.S. Veige, Polyhedron 27 (2008) 3177–3189;
f) M. Bortenschlager, J. Schutz, D. von Preysing, O. Nuyken, W.A. Herrmann, R. Weberskirch, J. Organomet. Chem. 23 (2004) 4817–4820;
g) E. Peris, R.H. Crabtree, Coord. Chem. Rev. 248 (2004) 2239–2284.
[7] S. Lotz, M. van den Berg, J.L. Dillen, Trans. Met. Chem. 13 (1988) 170–175.
[8] E.O. Fischer, F.J. Gammel, J.O. Besenhard, A. Frank, D. Neugebauer, J. Organomet. Chem. 191 (1980) 261–282.
[9] a) H. Kvapilová, I. Hoskovcová, J. Ludvík, S. Záliš, J. Heyrovsky, Organometallics 33 (2014) 4964–4972;
b) M. Landman, T. Levell, R. Pretorius, R. Fraser, B.E. Buitendach, M.M. Conradie, P.H. van Rooyen, J. Conradie, Electrochim. Acta 130 (2014) 104–118;
c) B. van der Westhuizen, P.J. Swarts, L.J. van Jaarsveld, D.C. Liles, U. Siegert, J.C. Swarts, I. Fernández, D.I. Bezuidenhout, Inorg. Chem. 52 (2013) 6674–6684;
d) G.M. Chu, A. Guerrero-Martínez, I. Fernández, M.A. Sierra, Chem. Eur J. 20 (2014) 1367–1375.
[10] a) C.A. Tolman, Chem. Rev. 77 (1977) 313–348;
b) T. Dröge, F. Glorius, Angew. Chem. Int. Ed. 49 (2010) 6940–6952;
c) S. Wolf, H.J. Plenio, J. Organomet. Chem. 694 (2009) 1487–1492.
[11] R.A. Kelly III, H. Clavier, S. Giudice, N.M. Scott, E.D. Stevens, J. Bordner, I. Samardjiev, C.D. Hoff, L. Cavallo, S.P. Nolan, Organometallics 27 (2008) 202–210.
[12] a) P. Veit, C. Volkert, C. Forster, V. Ksenofontrov, S. Schlicher, M. Bauer, K. Heinze, Chem. Commun. 55 (2019) 4615–4618;
b) S. Vanicek, M. Podewitz, J. Stubbe, D. Schulze, H. Kopacka, K. Wurst, T. Muller, P. Lippmann, S. Haslinger, H. Scholgenberger, K.R. Liedl, I. Ott, B. Sarkar, B. Bildstein, Chem. Eur J. 24 (2018) 3742–3753;
c) D. Aucamp, T. Witteler, F. Dielmann, S. Siangwata, D.C. Liles, G.S. Smih, D.I. Bezuidenhout, Eur. J. Inorg. Chem. (2017) 1227–1236;
d) S. Klenk, S. Rupf, L. Suntrup, M. van der Meer, B. Sarkar, Organometallics 36 (2017) 2026–2035.
[13] a) D.I. Bezuidenhout, B. van der Westhuizen, P.J. Swarts, T. Chatturgoon, O.Q. Munro, I. Fernandez, J.C. Swarts, Chem. Eur J. 20 (2014) 1–13;
b) B. van der Westhuizen, J.M. Speck, M. Korb, J. Friedrich, D.I. Bezuidenhout, H. Lang, Inorg. Chem. 52 (2013) 1423–14263;
c) D.I. Bezuidenhout, I. Fernandez, B. van der Westhuizen, P.J. Swarts, J.C. Swarts, Organometallics 32 (2013) 7334–7344.
[14] N.G. Connelly, W.E. Geiger, Chem. Rev. 96 (1996) 877–910.
[15] A. Hildebrandt, T. Ruffer, E. Erasmus, J.C. Swarts, H. Lang, Organometallics 29 (2010) 4900–4905.
[16] a) A. Kaemper, P. Kucmierczyk, T. Seidensticker, A.J. Vorholt, R. Franke, A. Behr, Cat. Sci. Tech. 6 (2016) 8072–8079;
b) L. Le Goaninvic, J.-L. Couturier, J.-L. Dubois, J.-F. Carpentier, J. Mol. Catal. A 417 (2016) 116–121;
c) M. Ali, A. Gual, G. Ebeling, J. Dupont, ChemCatChem 6 (2014) 2224–2228;
d) L. Wu, I. Fleischer, R. Jackstell, R. Profir, R. Franke, M. Beller, J. Am. Chem. Soc. 135 (2013) 14306–14312;
e) I. Fleischer, L. Wu, I. Profir, R. Jackstell, R. Franke, M. Beller, Chem. Eur J. 19 (2013) 10589–10594;
f) L. Alvila, T.A. Pakkanen, O. Krause, J. Mol. Catal. 84 (1993) 145–156.
[17] a) W. Gil, A.M. Trzeciak, J.J. Ziolkowski, Organometallics 27 (2008) 4131–4138;
b) M. Bortenschlager, J. Schutz, D. von Preysing, O. Nuyken, W.A. Herrmann, R. Weberskirch, J. Organomet. Chem. 690 (2005) 6233–6237.
[18] R.H. Crabtree, Chem. Rev. 112 (2012) 1536–1554.
[19] A.P.E.X.-3 Bruker, SAINT+, Version 6.02 (Includes XPREP and SADABS), Bruker AXS Inc., Madison, Wisconsin, USA, 2016.
[20] L.J. Farrugia, J. Appl. Crystallogr. 45 (2012) 849–854.
[21] G.M. Sheldrick, Acta Crystallogr. C. 71 (2015) 3–8.
[22] A.L. Spek, Acta Crystallogr. D. 65 (2009) 148–155.